

Early Proterozoic U-Pb Zircon Ages from Basement Gneiss at the Solovetsky Archipelago, White Sea, Russia

Stephan Schuth^{1*}, Victor I. Gornyy², Jasper Berndt³, Sergei S. Shevchenko⁴,
Sergei A. Sergeev⁴, Alexandr F. Karpuzov⁵, Tim Mansfeldt¹

¹Geographisches Institut, Bodengeographie/Bodenkunde, University of Cologne, Cologne, Germany

²Scientific Research Center for Ecological Safety, Russian Academy of Sciences, Saint-Petersburg, Russia

³Institut für Mineralogie, Westfälische Wilhelms-Universität Münster, Münster, Germany

⁴A. P. Karpinsky Russian Geological Research Institute (VSEGEI), Saint-Petersburg, Russia

⁵Federal Agency of Mineral Resources, Moscow, Russia

Email: *s.schuth@mineralogie.uni-hannover.de, v.i.gornyy@mail.ru, jberndt@uni-muenster.de,
Sergey_Shevchenko@vsegei.ru, karpuzov@rosnedra.com

Received December 5, 2011; revised January 25, 2012; accepted February 24, 2012

ABSTRACT

The central region of the Neoarchean Belomorian Mobile Belt (BMB) is, except for the Solovetsky Archipelago, largely covered by the White Sea. A newly discovered granitic gneiss outcrop on Solovetsky Island, Russia, enables a first age determination of the archipelago and evaluation of the hitherto poorly constrained central BMB. Zircons separated from the orthogneiss were analysed with SIMS-SHRIMP and LA-ICP-MS techniques. Both techniques yield a concordant U-Pb age of ca. 2.430 Ga, coinciding with ages of granitic intrusions in the BMB ca. 50 km west of the Solovetsky Islands.

Keywords: Solovetsky Archipelago; Granitic Gneiss Outcrop; Age Determination; 2.430 Ga

1. Introduction

The Neoarchean to Palaeoproterozoic Belomorian Mobile Belt (BMB) forms a SW-NE trending belt of mostly metamorphic rocks, which extends from northern Finland to the southern region of the Arkhangelsk Oblast in the Russian Federation (see e.g. [1], and inset of **Figure 1**). Located to the NE is the Neoarchean Murmansk Craton (comprising granodioritic and trondhjemitic orthogneisses), and the Kola Province (TTG-type orthogneisses of Neoarchean age). In the SW, the BMB borders the greenstone-granite domain of the Neoarchean Karelian Craton (e.g. [2]). The central area of the BMB is, except for the Solovetsky Archipelago, largely covered by the White Sea, making access to rocks a difficult task. The BMB consists of abundant TTG-type rocks (age ca. 2.9 Ga), and metavolcanic rocks of an age of ca. 1.9 Ga (e.g. [2-4]). The latter are associated with metasediments and a younger suite of granitic and gabbroic intrusions. Moreover, it was inferred that ca. 2.4 Ga old plutonic bodies are present in the BMB in significant proportions [4]. The Archaean units of the BMB were partially reworked during the Palaeoproterozoic Lapland-Kola collisional event ca. 1.9 Gyrs ago (e.g. [1,2], and references therein). Rifting at the Kandalaksha-Dvina aulacogen

crossing the western White Sea in SE-NW direction from the eastern Onega Peninsula to the Kandalaksha Bay started possibly in the late Palaeoproterozoic [1]. The aulacogen is segmented into grabens and horsts by several mostly WSW-ENE trending fault systems [5]. The oldest deposits in the grabens are volcanoclastic sediments, basic flows, and tuffs with a suggested age of ca. 1.8 - 1.4 Ga [5]. A simplified geological map is illustrated in the inset in **Figure 1**. A more detailed map and description of the BMB and Karelia is given by [6].

The Solovetsky Archipelago is located in the western White Sea, about 50 km east of the city of Kem' in Karelia and ca. 30 km NW of the Onega Peninsula (**Figure 1**). The island group consists of six large and several smaller islands with Bolshoi (Big) Solovetsky Island being the largest. About 50 km east of the archipelago, the Kandalaksha-Dvina aulacogen traverses the White Sea from SE to NW.

The first geological map (scale 1:200,000) of the archipelago was produced by [7], a section showing lithologies of the islands and the western coast of the White Sea is given in **Figure 1**. The islands are covered by glacial deposits derived most likely from the Kola Peninsula and the north-western areas of the BMB. The last glaciation of the archipelago occurred in the late Pleistocene

*Corresponding author.

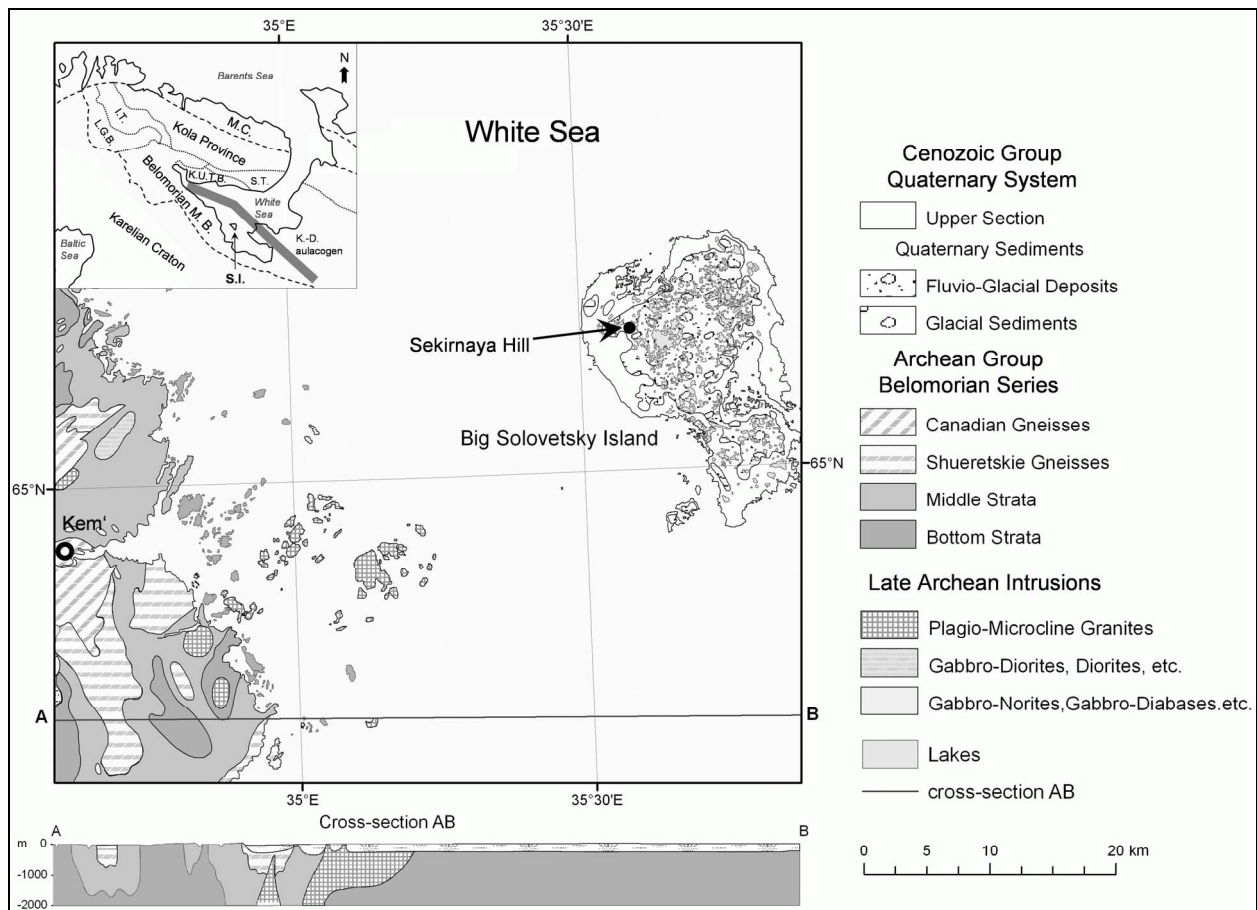


Figure 1. Simplified tectonic and geological overview of the White Sea region and the Solovetsky Archipelago. The inset shows the boundaries of the different provinces in NE Fennoscandia (modified after [2]). I. T.: Inari Terrane; K. U. T. B.: Kolvitsa-Umba-Tersk Belt; L. G. B.: Lapland Granulite Belt; M. C.: Murmansk Craton; S. T.: Strelna Terrane; K.-D.: Kandalaksha-Dvina aulacogen (solid grey line); S. I.: Solovetsky Islands. The map shows strata of the Belomorian Mobile Belt around the city of Kem' and the Solovetsky Islands (after [7]). Bolshoi (Big) Solovetsky Island is characterized by numerous lakes of different sizes and glacial deposits. The sample location at the slope of the Sekirnaya Hill is shown by the black dot.

during the Valdai glaciation (e.g. [8]). A Neoproterozoic basement (labelled “Bottom Strata” in **Figure 1**) with an age of ca. 2.6 - 2.2 Ga was suggested by [7] to be present beneath the islands. Moreover, the archipelago is directly located on two WSW-ENE trending zones marked by local late Archaean granitic intrusions [7]. In addition, gravimetric, seismic, and geoelectrical data recorded on Bolshoi Solovetsky by [9] revealed that the crust is thinnest (ca. 28 km) in comparison to the surrounding area, and a mantle diapir of unknown age is situated beneath the islands. Devonian magmatic activity in the western White Sea region was likely initiated by an upwelling mantle plume, as suggested by [10], and [11] on the basis of tectonic interpretation of satellite images. This triggered an uplift of the area and may still support present-day weak local positive thermal anomalies observed in lakes and soils, and formation of an extrazonal thermophilic ecosystem on Bolshoi Solovetsky Island [12,13].

In July 2009, a group of Russian and German geolo-

gists and geophysicists discovered on this island a gneiss outcrop which is probably related to the BMB. The outcrop (ca. 7.5 × 5 m) is located at the lower flanks of Sekirnaya Hill in the north-western part of the island (**Figure 1**). It consists of relatively fresh granitic gneiss. Other lithologies were not found in the outcrop. This provides an opportunity of a first age determination of the basement of the archipelago and, in a broader context, may help to elucidate the geological evolution of the central region of the BMB. The orthogneiss was dated via the U-Pb zircon dating method employed to two different instrumental techniques (SIMS-SHRIMP and LA-ICP-MS).

2. Methods

The orthogneiss sample (labelled “R1”) from Bolshoi Solovetsky Island was sawed into smaller pieces for thin section preparation, crushing in a jaw breaker and steel

mortar. From the crushed sample, a part was ground to powder for X-ray Fluorescence (XRF) analysis employing an ARL 9800 instrument at VSEGEI. The XRF data were further processed via CIPW norm for sample classification.

Another representative portion of the crushed material was used for separation of accessory zircon which was required for comparative age determination in different laboratories using SIMS (Secondary Ion Mass-Spectrometry) by Sensitive High-Resolution Ion Micro Probe (SHRIMP-II, at the Centre of Isotopic Research of VSEGEI, St. Petersburg, Russia) and Laser Ablation-Sector Field-Inductively Coupled Plasma-Mass Spectrometry technique (LA-SF-ICP-MS, at the Institute for Mineralogy, University of Münster, Germany), respectively. In addition of dating a hitherto unknown outcrop in a geologically complex region, the two involved institutions were able to compare their respective techniques by using well-defined standards and unknown zircons. The separation procedures employed in the Russian and German laboratories are given in **Table 1**.

For analyses, selected zircon grains were mounted in Pb-free epoxy resin together with the TEMORA 1, GJ-1, and/or 91500 reference zircons. The grains were sectioned approximately in half, polished and coated. Cathodoluminescence (CL) images were used to reveal the internal structures of the zircon grains and thereby define target areas within them. The technical methods applied in the different institutions are given in **Table 1**.

2.1. SHRIMP Analyses

The results were obtained with a secondary electron multiplier operated in peak-jumping mode, as outlined by [14]. A primary beam of molecular oxygen was employed to bombard the zircons in order to extract secondary ions. A 70 μm Kohler aperture allowed focusing of the primary beam so that the ellipse-shaped analytical spot had a size ca 25 \times 20 μm . The sputtered secondary ions were accelerated at 10 kV. A mass-resolution of $M/\Delta M \geq 5000$ (1% valley definition) was achieved via an 80 μm wide slit of the secondary ion source combined with a 100 μm multiplier slit; thus, all possible isobaric interferences were resolved. Rastering for one minute over a rectangular area of ca. 65 \times 50 μm before each analysis removed the gold coating and any possible surface common-Pb contamination.

The ion species of interest were measured in a sequence as follows: $^{196}\text{(Zr}_2\text{O)}\text{-}^{204}\text{Pb}$ -background (ca. 204 a.m.u.)- ^{206}Pb - ^{207}Pb - ^{208}Pb - ^{238}U - ^{248}ThO - ^{254}UO with integration times ranging from 2 s to 14 s. Seven cycles for each analyzed spot were acquired. Apart from “unknown” zircons, each fourth measurement was carried out on the zircon Pb/U standard TEMORA 1, which has an ac-

Table 1. The table lists the different analytical techniques used for this study.

Technique by country	Germany	Russia
Separation technique	Hand magnet, sieving, CH_2I_2 heavy liquid, Frantz magnetic separator, hand-picking ¹	Sieving, separation table, CH_2I_2 heavy liquid, Frantz magnetic separator, hand-picking ³
Grain fraction used	63 - 125 μm	100 - 150 μm
Microprobe/SEM for CL images	JEOL JXA 8200 ¹	CamScan MX 2500 ³
Coating, voltage, and current	Carbon, 15 kV, 15 nA	Gold, 15 kV, 10 nA
Analytical technique	LA-SF-ICP-MS	SIMS-SHRIMP
Instrument	Thermo-Finnigan Element 2 ²	SHRIMP-II ³
Beam type	New Wave ArF Excimer laser ²	O_2^- , 5 nA
Energy	ca. 5 Jcm^{-2}	10 kV (2 nd acceleration)
Spot size (number of analyses)	35 μm (n = 92), 25 μm (n = 23)	ellipse 20 \times 25 μm
Analysis time per spot	20 ns (pulse), 10 Hz (repetition)	ca. 6 min
Number of analyses	115	10
Discarded results	17	0
Analyses \geq 95% concordance	70	10
Reference zircons	91500	91500
U-Pb age of 91500	1072 Ma \pm 11 Ma (2 σ , n = 5)	1066 Ma \pm 7 Ma (2 σ , n = 6)
U-Pb zircon age of R1	2429.1 Ma \pm 9.3 Ma (2 σ)	2433 Ma \pm 13 Ma (2 σ)
MSWD	5.5	0.089

¹Steinmann Institute at University of Bonn; ²Institute of Mineralogy at University of Münster; ³A. P. Karpinsky Russian Geological Research Institute (VSEGEI), St. Petersburg.

cepted $^{206}\text{Pb}/^{238}\text{U}$ age of 416.75 \pm 0.24 Ma [15]. The 91500 zircon standard (U = 81.2 ppm, $^{206}\text{Pb}/^{238}\text{U}$ age = 1062.4 \pm 0.4 Ma; [16]) was applied as a U-concentration standard. The Pb-U ratios have been normalized relative to a value of 0.0668 for $^{206}\text{Pb}/^{238}\text{U}$ of the TEMORA 1 reference zircons. Error in TEMORA standard calibration was 0.62%. The results were then processed with the SQUID 1.02 (see [17]) and Isoplot/Ex 3.00 (see [18]) software, using the decay constants of [19]. The common Pb correction was done on the basis of measured ^{204}Pb and present-day Pb isotope composition, according to the model of [20].

2.2. LA-ICP-MS Analyses

The U-Pb age determinations were done using a LA-SF-ICP mass spectrometer (Element 2, ThermoFinnigan) and a New Wave ArF Excimer Laser system at Univer-

sity of Münster, Germany. Forward power was 1330 W, gas flow rates were about 0.7 L/min for He (employed as carrier gas for ablated material), and 0.9 L/min and 1 L/min for the Ar auxiliary and sample gas, respectively. The cooling gas flow rate was set to 16 L/min. Before starting the analyses, the system has been tuned on the standard reference material SRM 612 from the NIST (National Institute of Standards and Technology) by measuring ^{139}La , ^{232}Th , and $^{232}\text{Th}^{16}\text{O}$ to get stable signals and a high sensitivity on ^{139}La and ^{232}Th peaks, as well as low oxide rates ($^{232}\text{Th}^{16}\text{O}/^{232}\text{Th} \sim 0.1\%$) during ablation. The repetition rate was 10 Hz at an energy of $\sim 5 \text{ J/cm}^2$. The typical spot size was $35 \mu\text{m}$, in some cases also $25 \mu\text{m}$.

For U-Pb analyses of the zircons, the masses ^{204}Pb , ^{206}Pb , ^{207}Pb , and ^{238}U were measured. In addition, ^{202}Hg was analyzed to correct the interference of ^{204}Hg on ^{204}Pb , which is important to apply, if necessary, for a common-Pb correction. The common Pb proportion for the individual spots is calculated from the ^{204}Hg -corrected ^{204}Pb signal, applying the two-stage model of [20]. When the contribution of estimated common ^{206}Pb to the total ^{206}Pb exceeded 1%, which corresponds approximately to the analytical uncertainty of the measured Pb isotope ratios, a common Pb correction was applied. Ten unknown samples were bracketed with three calibration standards (GJ-1; [21]) to correct for instrumental mass bias. The sensitivity for measured Pb and U isotopes for a $35 \mu\text{m}$ spot was typically in the range of 4000 cps/ppm. Age calculations were done with an in-house Microsoft[®] Excel spreadsheet using the intercept method (e.g. [22]) to correct for elemental fractionation during laser analyses. Along with the samples, the 91500 zircon standard was measured to monitor accuracy and precision of the analyses. A three-shot pre-ablation was applied to all spots to remove the carbon coating and potential common Pb contamination from the surface. Out of 111 embedded zircons, 98 were selected for analyses after inspection of CL images. Cracks and inclusions were avoided. In total, 115 measurements were carried out.

3. Results

3.1. Petrography

Sample R1 is a medium-grained foliated granitic gneiss with abundant orthoclase and amphibole. Hand specimen and thin section inspection yielded a composition of ca. 45 vol% of feldspar, 25 vol% of amphibole, 25 vol% of quartz, ca. 5 vol% biotite, and accessory phases like garnet, apatite, zircon, and opaque phases. Results of XRF analyses are given in **Table 2**, classifying the sample as an acid alkaline rock because of its high silica and alkali content. As illustrated in **Figure 2**, ternary classification schemes after [23] and [24] indicate (syeno-)granite

Table 2. Major element composition of the gneiss sample (XRF data). Total iron as Fe_2O_3 . LOI: Loss on ignition.

	wt%		wt%
SiO_2	67.0	CaO	3.13
Al_2O_3	12.3	Na_2O	2.59
TiO_2	1.33	K_2O	4.22
$\text{Fe}_2\text{O}_3^{\dagger}$	7.11	P_2O_5	0.37
MnO	0.10	LOI	0.43
MgO	1.31	Sum	99.9

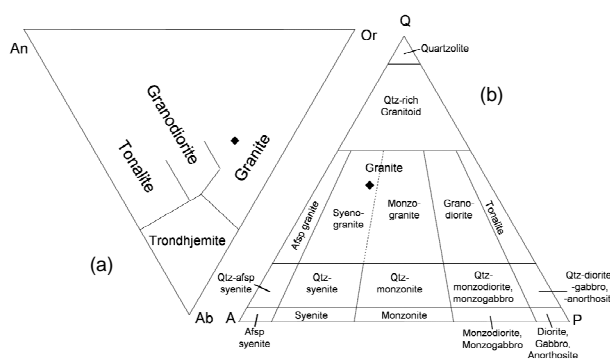


Figure 2. Classification of the gneiss R1 after [23] (a), and [24] (b), respectively. Proportions of albite (Ab), anorthite (An), orthoclase (Or), alkali feldspar (A, Afsp), quartz (Q, Qtz), and plagioclase (P) were calculated after the CIPW norm. Both schemes suggest a granite precursor rock.

as a precursor rock for R1. Therefore, R1 is classified as an orthogneiss (metasyenogranite). In addition, low MgO-CaO (0.42) and high $\text{P}_2\text{O}_5\text{-TiO}_2$ (0.28) ratios suggest a magmatic origin of the precursor rock [25].

The zircons are largely present as short prismatic and prismatic crystals with a length-wide ratio of ca. 1.5 to 3. Facets of prisms and pyramids are distinct, but show sometimes signs of chemical corrosion. Small, sporadic mineral and gas-liquid inclusions are observed under a binocular. In addition, the zircons of R1 often show well developed oscillatory zoning, which is sometimes present as sector zoning and is considered a typical feature of magmatic zircons (e.g. [26], and references therein). Some examples are shown as CL images in **Figure 3**.

3.2. SHRIMP Results

All ten *in situ* U-Pb isotopic analyses on eight typical zircon grains, free of cracks and inclusions, gave a well-defined concordant age. The results of the zircon analyses are shown in **Table 3** and **Figure 4(a)**. During the course of this study, the 91500 standard zircon yielded a $^{207}\text{Pb}/^{206}\text{Pb}$ age of $1066 \pm 7 \text{ Ma}$ ($n = 6$). The zircons are characterized by an average Th-U ratio scattering around 0.77, and low contents of uranium (average 47 ppm), and thorium (average 36 ppm). Concentrations of non-radio-

Table 3. Results of the SIMS-SHRIMP analyses. Errors are 1σ ; Pb_c and Pb^* indicate the common and radiogenic proportions, respectively. The error for the Temora standard calibration was 0.62% (not included in above errors but required when comparing data from different mounts). The correction for common Pb was done by using measured ^{204}Pb according to the model of [20].

Spot	% $^{206}Pb_c$	ppm U	ppm Th	$^{232}Th/^{238}U$	ppm $^{206}Pb^*$	$^{206}Pb/^{238}U$ Age	$^{207}Pb/^{206}Pb$ Age	% Disc.	Total $^{238}U/^{206}Pb$ $\pm\%$	Total $^{207}Pb/^{206}Pb$ $\pm\%$	$^{238}U/^{206}Pb^*$ $\pm\%$	$^{207}Pb^*/^{206}Pb^*$ $\pm\%$	$^{207}Pb^*/^{235}U$ $\pm\%$	$^{206}Pb^*/^{238}U$ $\pm\%$	Err. corr.						
C-1.1.1	0.42	37	25	0.69	14.5	2421 \pm 31	2430 \pm 46	0	2.182	1.4	0.1613	1.6	2.191	1.5	0.1576	2.7	9.91	3.1	0.4558	1.5	0.49
C-1.1.2	0.26	58	52	0.92	22.6	2397 \pm 25	2413 \pm 26	1	2.213	1.2	0.1584	1.3	2.218	1.3	0.1560	1.5	9.69	2.0	0.4504	1.3	0.64
C-1.2.1	0.54	31	26	0.89	11.9	2395 \pm 33	2397 \pm 38	0	2.207	1.6	0.1594	1.6	2.219	1.7	0.1546	2.2	9.59	2.8	0.4499	1.7	0.60
C-1.3.1	0.26	18	11	0.63	7.50	2497 \pm 42	2408 \pm 38	-4	2.107	2.0	0.1578	2.0	2.112	2.0	0.1555	2.2	10.2	3.0	0.4731	2.0	0.67
C-1.3.2	0.11	42	38	0.92	16.9	2450 \pm 28	2449 \pm 23	0	2.160	1.4	0.1604	1.3	2.162	1.4	0.1594	1.4	10.2	1.9	0.4623	1.4	0.71
C-1.4.1	0.03	153	116	0.78	61.0	2456 \pm 20	2456 \pm 15	0	2.156	0.96	0.1603	0.86	2.156	0.96	0.1600	0.87	10.2	1.3	0.4637	0.96	0.74
C-1.5.1	0.00	37	25	0.70	14.5	2440 \pm 31	2427 \pm 28	-1	2.173	1.5	0.1573	1.7	2.173	1.5	0.1573	1.7	9.98	2.3	0.4602	1.5	0.67
C-1.6.1	0.44	41	31	0.76	16.0	2386 \pm 29	2408 \pm 32	1	2.220	1.4	0.1595	1.6	2.229	1.5	0.1556	1.9	9.61	2.4	0.4479	1.5	0.61
C-1.7.1	0.57	31	23	0.77	12.5	2481 \pm 35	2439 \pm 40	-2	2.114	1.7	0.1636	1.8	2.126	1.7	0.1585	2.4	10.3	2.9	0.4695	1.7	0.58
C-1.8.1	0.45	26	17	0.66	10.2	2397 \pm 36	2428 \pm 41	1	2.207	1.8	0.1615	2.0	2.217	1.8	0.1575	2.4	9.78	3.0	0.4504	1.8	0.60

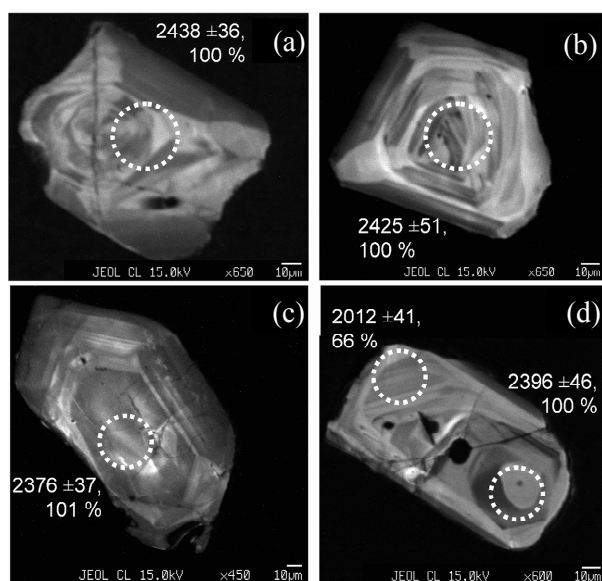


Figure 3. CL images of four zircons (a)-(d). Laser spots are highlighted as dashed white circles, ages ($^{207}Pb/^{235}U$ in Ma, $\pm 2\sigma$) and the degree of concordance is given for comparison. Sector zoning is visible in (a) and (b); Less developed zoning and a non-zoned core region marks the crystal in (c); The zircon shown in (d) exhibits slight resorption at the boundary beneath the left laser spot. It also yielded different ages for core and rim, respectively.

genic lead are insignificant ($<0.5\%$). Zircon cores as well as metamorphic overgrowths or rims were not found. Such geochemical features are commonly observed for zircons in magmatic rocks (e.g. [26,27]), but are not always a positive proof (for further discussion, see [28]). For age calculation, all analytical results were used without discrimination. As a result, SHRIMP analyses of eight R1 zircons yield a concordant age of 2433 ± 13 Ma (2σ).

3.3. LA-ICP-MS Results

Analyses of the standard zircon 91500 (see **Figure 5**) gave an $^{206}Pb/^{238}U$ age of 1072 ± 11 Ma (2σ , $n = 5$) which is in agreement with earlier reports (e.g. [16]: 1062.4 ± 0.4 Ma; [29]: 1061.3 ± 4.3 Ma, and references therein). As is evident from **Figure 4(b)**, most zircons analysed with LA-ICP-MS give an upper intercept age of 2429.1 ± 9.3 Ma (2σ , $n = 70$, degree of concordance $\geq 95\%$). However, for the remaining results, loss of Pb by later processes seems to have affected some of the zircons because of their lower Pb-U isotope ratios. These discordant ages ($n = 28$) were obtained mostly for the rims of the analysed zircons. Of the 115 analyzed spots, 17 results were discarded because the signal intensity was too low or dropped too fast (*i.e.*, the chosen spot did not offer a sufficient amount of zircon material for analy-

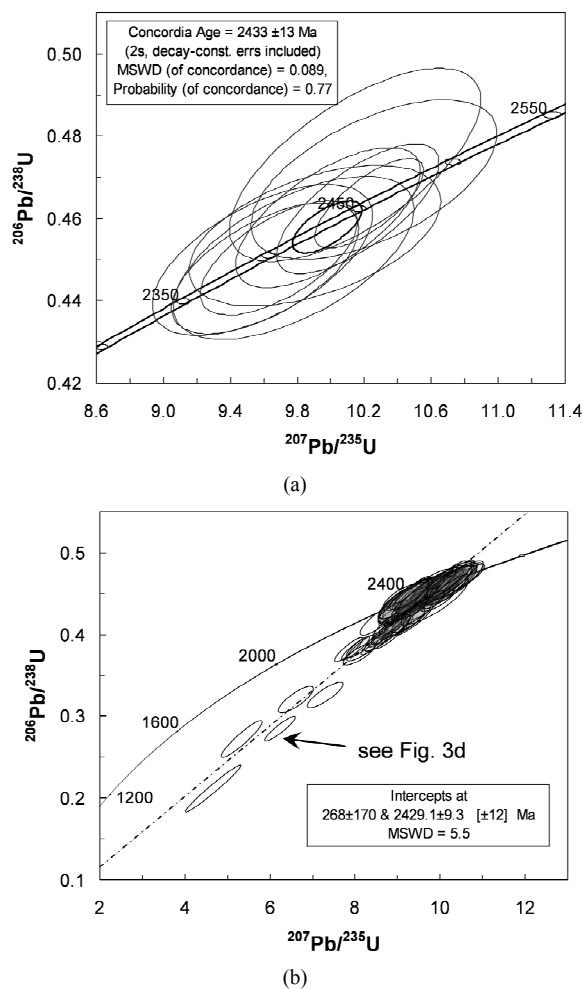


Figure 4. U-Pb concordia diagrams for zircons analysed by SIMS-SHRIMP-II (a) and LA-ICP-MS (b), respectively. The data point ellipses correspond to 2σ uncertainty. In (b), the arrow marks the result of the rim analysis of the zircon shown in Figure 3(d), and the stippled line represents the discordia line. The upper intercept gives an age of 2.429 Ga.

sis). The complete LA-ICP-MS data set is available upon request.

4. Discussion

The geological complexity of the Belomorian Mobile Belt (BMB) in NW Russia has been known for several years (e.g. [4,30]). However, little data with respect to lithologies and rock ages are so far available for the White Sea region that covers large parts of the central BMB section. We show here that a hitherto unknown gneiss outcrop on Solovetsky Island in the western White Sea is related to granitic intrusions in the central BMB and yields a U-Pb zircon age of ca. 2.43 Ga. This age was achieved independently via SHRIMP and LA-ICP-MS, again confirming the reliability of these methods as already shown by previous studies (e.g. [31]).

The composition of the orthogneiss R1 (a metasyenogranite) and its U-Pb zircon age coincide with granitic intrusions observed for the western BMB at ca. 2.4 Ga (e.g. [4,32]). This new age information strongly suggests magmatic activity at 2.43 Ga in the central section of the BMB where it was unknown so far because of missing accessible outcrops. Moreover, the granitic gneiss of Solovetsky Island is located on the convergence of two SW-NE trending zones of variably sized granite intrusions as suggested by [7] in a pioneering geological study of the western BMB region around the city of Kem' (Figure 1). The nature, origin, and extension of these zones of granitic intrusions especially further east are still uncertain. To note, charnockites to the west and SW of Kem' yield a U-Pb zircon age of 2.4 to 2.45 Ga as well [32]. Taken together, the central and western region of the BMB was affected by granitic intrusions at ca. 2.4 Ga, however, the magma compositions varied on a local scale (e.g., charnockites, syenogranites). Potassium-Ar ages of the granites reported by [7] range from 1.86 to 1.93 Ga. These age data coincide with the Lapland-Kola collisional event at ca. 1.9 Ga that has obviously reset the granite K-Ar age due to metamorphism (e.g. [1,2]). Interestingly, some zircons analysed with LA-ICP-MS yield lower discordant U-Pb ages at their rims (Figure 3(d)). Again, this is in agreement with the time of metamorphic events; however, we cannot exclude multiple episodes of Pb loss as is tentatively suggested by a few discordant zircon ages of lower than 2.4 Ga. The influence of the mantle diapir on the U-Pb isotope composition of the zircons (Pb loss due to re-heating, or younger zircon growth during ascent of hydrothermal fluids) is difficult to evaluate. The lower intercept age given in Figure 4(b) is poorly constrained at 268 Ma ± 170 Ma because of the scarcity of zircons with a discordant U-Pb age. However, it still coincides within analytical uncertainty with the time of Devonian magmatic activity in the western White Sea region (e.g. [10]). The offset of the U-Pb age of some R1 zircons may result from ascending hydrothermal fluids and subsequent Pb loss and/or overgrowth. In contrast, [11] suggested on the basis of geothermal data and geophysical modelling that the last tectono-magmatic activity in the central BMB took place during early Miocene. In summary, the mantle diapir has likely affected the central BMB region in Phanerozoic time, but the extension and intensity of magmatic activity still remains uncertain.

Composition and age of the rock units forming the BMB can vary on a scale of sometimes a few meters (e.g. [4,30,33]); hence it is possible that a complex basement is situated beneath the cover of glacial deposits at the Solovetsky archipelago. As the geological map given by [6] is of a scale of 1:4,000,000, and the map of [7] lacks detailed information about magmatic rocks, thorough

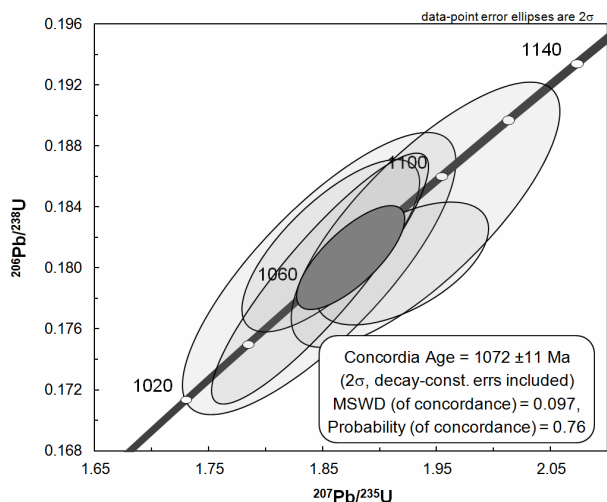


Figure 5. U-Pb concordia diagram for the zircon standard 91500 analysed by LA-ICP-MS in Münster, Germany. The result is in agreement with earlier reports (e.g. [16]: 1062.4 ± 0.4 Ma; [29]: 1061.3 ± 4.3 Ma).

geological mapping and dating of possible other rock units of outcropping basement material at the islands may uncover a possibly complex geology. The mantle diapir beneath the island group likely facilitated rise of the islands above sea level [9], and, in conjunction with an extrazonal ecosystem characterized by thermophilic vegetation close to the polar circle [12,13,34], highlights a special geotectonic setting and possible modern tectonic activation to be investigated further.

5. Acknowledgements

From University of Bonn, S. Jahn-Awe kindly assisted with heavy liquid separation and zircon picking, and R. Spiering is thanked for supervision of CL imaging. From University of Cologne, R. Kleinschrodt is thanked for coating of the epoxy mounts, and P. Garcia for thin section preparation. This study was funded jointly by the DFG (German Research Foundation) by grant Ma2143-10 to T. M. and the Russian Foundation for Basic Research to V. G. by grant 09-05-91360-NNIO_g as a part of the project “Energy Supply of Extrazonal Ecosystems”. We thank A. Zeh and S. Daly for constructive comments on an earlier version of the manuscript.

REFERENCES

- [1] S. V. Bogdanova, B. Bingen, R. Gorbatshev, T. N. Kheraskova, V. I. Kozlov, V. N. Puchkov, *et al.*, “The East European Craton (Baltica) before and during the Assembly of Rodinia,” *Precambrian Research*, Vol. 160, No. 1-2, 2008, pp. 23-45. [doi:10.1016/j.precamres.2007.04.024](https://doi.org/10.1016/j.precamres.2007.04.024)
- [2] J. S. Daly, V. V. Balagansky, M. J. Timmerman and M. J. Whitehouse, “The Lapland-Kola Orogen: Palaeoproterozoic Collision and Accretion of the Northern Fennoscandian Lithosphere,” In: D. G. Gee and R. A. Stephenson, Eds., *European Lithosphere Dynamics, The Geological Society London, Memoirs*, London, Vol. 32, 2006, pp. 579-598.
- [3] A. I. Tugarinov and E. V. Bibikova, “Geochronology of the Baltic Shield by Zircon Determinations,” Nauka, Moscow, 1980.
- [4] S. V. Bogdanova and E. V. Bibikova, “The ‘Saamian’ of the Belomorian Mobile Belt: New Geochronological Constraints,” *Precambrian Research*, Vol. 64, No. 1-4, 1993, pp. 131-152. [doi:10.1016/0301-9268\(93\)90072-A](https://doi.org/10.1016/0301-9268(93)90072-A)
- [5] T. N. Kheraskova, R. B. Sapozhnikov, Yu. A. Volozh and M. P. Antipov, “Geodynamics and Evolution of the Northern East European Platform in the Late Precambrian as Inferred from Regional Seismic Profiling,” *Geotectonics*, Vol. 40, 2006, pp. 434-449. [doi:10.1134/S0016852106060021](https://doi.org/10.1134/S0016852106060021)
- [6] M. Mints, A. Suleimanov, N. Zamozhniaya and V. Stupak, “A Three-Dimensional Model of the Early Precambrian Crust under the Southeastern Fennoscandian Shield: Karelia Craton and Belomorian Tectonic Province,” *Tectonophysics*, Vol. 472, No. 1-4, 2009, pp. 323-339. [doi:10.1016/j.tecto.2008.12.008](https://doi.org/10.1016/j.tecto.2008.12.008)
- [7] V. I. Shmygalev, H. M. Shmygaleva and M. A. Korsakov, “Geological Map of the USSR, Scale: 1:200,000,” In: K. A. Shurkin, Ed., *Karelian Series*, Q-36-XXIX, XXX, State Geological Committee of the USSR, Moscow, 1962.
- [8] A. A. Velichko, M. A. Faustova, Y. N. Gribchenko, V. V. Pisareva and N. G. Sudakova, “Glaciations of the East European Plain—Distribution and Chronology,” In: J. Ehlers and P. L. Gibbard, Eds., *Quaternary Glaciations—Extent and Chronology, Part I: Europe*, Elsevier, Amsterdam, 2004, pp. 337-354.
- [9] Yu. G. Shvartsman, “Deep Structure,” In: Yu. G. Shvartsman and I. N. Bolotov, Eds., *Natural Environment of the Solovetsky Archipelago under a Changing Climate*, The Ural Division of the Russian Academy of Sciences, Yekaterinburg, 2007, pp. 23-25.
- [10] H. Downes, E. Balaganskaya, A. Beard, R. Liferovich and D. Demaiffe, “Petrogenetic Processes in the Ultramafic, Alkaline and Carbonatitic Magmatism in the Kola Alkaline Province: A Review,” *Lithos*, Vol. 85, No. 1-4, 2005, pp. 48-75. [doi:10.1016/j.lithos.2005.03.020](https://doi.org/10.1016/j.lithos.2005.03.020)
- [11] V. I. Gornyi, “The Mantle Convection and the Drift of Euro-Asian Plate (According the Remote Geothermal Method Data),” *Geoscience and Remote Sensing Symposium, 2002 IEEE International*, Vol. 4, 2002, pp. 2029-2035.
- [12] Yu. G. Shvartsman and I. N. Bolotov, “Mechanisms of Extrazonal Biocoenosis Formation at the Solovetsky Islands,” *Ecologia*, Vol. 5, 2005, pp. 344-352.
- [13] V. I. Gornyy, “Thermal Conditions of Lakes,” In: Yu. G. Shvartsman and I. N. Bolotov, Eds., *Natural Environment of the Solovetsky Archipelago under a Changing Climate*, The Ural Division of the Russian Academy of Sciences, Yekaterinburg, 2007, pp. 63-66.
- [14] I. S. Williams, “U-Th-Pb Geochronology by Ion Micro-

- probe,” In: M. A. McKibben, W. C. Shanks III and W. I. Ridley, Eds., *Applications of Microanalytical Techniques to Understanding Mineralizing Processes*, Society of Economic Geologists, Littleton, 1998, pp. 1-35.
- [15] L. P. Black, S. L. Kamo, C. M. Allen, J. N. Aleinikoff, D. W. Davis, R. J. Korsch, *et al.*, “TEMORA 1: A New Zircon Standard for Phanerozoic U-Pb Geochronology,” *Chemical Geology*, Vol. 200, 2003, pp. 155-170. [doi:10.1016/S0009-2541\(03\)00165-7](https://doi.org/10.1016/S0009-2541(03)00165-7)
- [16] M. Wiedenbeck, P. Allé, F. Corfu, W. L. Griffin, M. Meier, F. Oberli, A. von Quadt, *et al.*, “Three Natural Zircon Standards for U-Th-Pb, Lu-Hf, Trace Element and REE Analyses,” *Geostandards Newsletter*, Vol. 19, No. 1, 1995, pp. 1-23. [doi:10.1111/j.1751-908X.1995.tb00147.x](https://doi.org/10.1111/j.1751-908X.1995.tb00147.x)
- [17] K. R. Ludwig, “SQUID 1.02, a User Manual, a Geochronological Toolkit for Microsoft Excel,” Berkeley Geochronology Center Special Publication, Berkeley, 2001.
- [18] K. R. Ludwig, “User’s Manual for Isoplot/Ex, Version 3.00, A Geochronological Toolkit for Microsoft Excel,” Berkeley Geochronology Center Special Publication, Berkeley, 2003.
- [19] R. H. Steiger and E. Jäger, “Subcommission on Geochronology: Convention on the Use of Decay Constants in Geo- and Cosmochronology,” *Earth and Planetary Science Letters*, Vol. 36, No. 3, 1977, pp. 359-362. [doi:10.1016/0012-821X\(77\)90060-7](https://doi.org/10.1016/0012-821X(77)90060-7)
- [20] S. Stacey and J. D. Kramers, “Approximation of Terrestrial Lead Isotope Evolution by a Two-Stage Model,” *Earth and Planetary Science Letters*, Vol. 26, 1975, pp. 207-221. [doi:10.1016/0012-821X\(75\)90088-6](https://doi.org/10.1016/0012-821X(75)90088-6)
- [21] S. E. Jackson, N. J. Pearson, W. L. Griffin and E. A. Belousova, “The Application of Laser Ablation-inductively Coupled Plasma-Mass Spectrometry to *in Situ* U-Pb Zircon Geochronology,” *Chemical Geology*, Vol. 211, No. 1-2, 2004, pp. 47-69. [doi:10.1016/j.chemgeo.2004.06.017](https://doi.org/10.1016/j.chemgeo.2004.06.017)
- [22] J. Košler and P. J. Sylvester, “Present Trends and the Future of Zircon in Geochronology: Laser Ablation ICPMS,” *Reviews in Mineralogy and Geochemistry*, Vol. 53, No. 1, 2003, pp. 243-275. [doi:10.2113/0530243](https://doi.org/10.2113/0530243)
- [23] F. Barker, “Trondhjemite: Definition, Environment and Hypotheses of Origin,” In: F. Barker, Ed., *Trondhjemites, Dacites, and Related Rocks*, *Developments in Petrology*, Vol. 6, 1979, pp. 1-12.
- [24] A. Streckeisen, “To Each Plutonic Rock Its Proper Name,” *Earth-Science Reviews*, Vol. 12, No. 1, 1976, pp. 1-33. [doi:10.1016/0012-8252\(76\)90052-0](https://doi.org/10.1016/0012-8252(76)90052-0)
- [25] C. D. Werner, “Saxonian Granulites—Igneous or Lithogenous. A Contribution to the Geochemical Diagnosis of the Original Rocks in High-Metamorphic Complexes,” *ZfS-Mitteilungen*, Vol. 133, 1987, pp. 221-250.
- [26] P. W. O. Hoskin and U. Schaltegger, “The Composition of Zircon and Igneous and Metamorphic Petrogenesis,” *Reviews in Mineralogy and Geochemistry*, Vol. 53, No. 1, 2003, pp. 27-62. [doi:10.2113/0530027](https://doi.org/10.2113/0530027)
- [27] F. Tomaschek, A. K. Kennedy, I. M. Villa, M. Lagos and C. Ballhaus, “Zircons from Syros, Cyclades, Greece—Recrystallization and Mobilization of Zircon during High-Pressure Metamorphism,” *Journal of Petrology*, Vol. 44, No. 11, 2003, pp. 1977-2002. [doi:10.1093/petrology/egg067](https://doi.org/10.1093/petrology/egg067)
- [28] B. Fu, T. P. Mernagh, N. T. Kita, A. I. S. Kemp and J. W. Valley, “Distinguishing Magmatic Zircon from Hydrothermal Zircon: A Case Study from the Gidginbung High-Sulphidation Au-Ag-(Cu) Deposit, SE Australia,” *Chemical Geology*, Vol. 259, 2009, pp. 131-142. [doi:10.1016/j.chemgeo.2008.10.035](https://doi.org/10.1016/j.chemgeo.2008.10.035)
- [29] Y. Nebel-Jacobsen, E. E. Scherer, C. Münker and K. Mezger, “Separation of U, Pb, Lu, and Hf from Single Zircons for Combined U-Pb Dating and Hf Isotope Measurements by TIMS and MC-ICPMS,” *Chemical Geology*, Vol. 220, No. 1-2, 2005, pp. 105-120. [doi:10.1016/j.chemgeo.2005.03.009](https://doi.org/10.1016/j.chemgeo.2005.03.009)
- [30] V. V. Balagansky, M. J. Timmerman, N. Y. Kozlova and R. V. Kislitsyn, “A 2.44 Ga Syn-Tectonic Mafic Dyke Swarm in the Kolvitsa Belt, Kola Peninsula, Russia: Implications for Early Palaeoproterozoic Tectonics in the North-Eastern Fennoscandian Shield,” *Precambrian Research*, Vol. 105, No. 2, 2001, pp. 269-287. [doi:10.1016/S0301-9268\(00\)00115-7](https://doi.org/10.1016/S0301-9268(00)00115-7)
- [31] A. Gerdes and A. Zeh, “Combined U-Pb and Hf Isotope LA-(MC-)ICP-MS Analyses of Detrital Zircons: Comparison with SHRIMP and New Constraints for the Provenance and Age of an Armorican Metasediment in Central Germany,” *Earth and Planetary Science Letters*, Vol. 249, 2006, pp. 47-61. [doi:10.1016/j.epsl.2006.06.039](https://doi.org/10.1016/j.epsl.2006.06.039)
- [32] E. Bibikova, T. Skiöld, S. Bogdanova, R. Gorbatshev and A. Slabunov, “Titanite-Rutile Thermochronometry Across the Boundary between the Archaean Craton in Karelia and the Belomorian Mobile Belt, Eastern Baltic Shield,” *Precambrian Research*, Vol. 105, 2001, pp. 315-330. [doi:10.1016/S0301-9268\(00\)00117-0](https://doi.org/10.1016/S0301-9268(00)00117-0)
- [33] S. B. Lobach-Zuchenko, N. A. Arestova, V. P. Chekulaev, L. K. Levsky, E. S. Bogomolov and I. N. Krylov, “Geochemistry and Petrology of 2.40 - 2.45 Ga Magmatic Rocks in the North-Western Belomorian Belt, Fennoscandian Shield, Russia,” *Precambrian Research*, Vol. 92, 1998, pp. 223-250. [doi:10.1016/S0301-9268\(98\)00076-X](https://doi.org/10.1016/S0301-9268(98)00076-X)
- [34] V. I. Gornyy, “Distribution of Convective Heat Flow in the White Sea Region According to the Data of a Remote Geothermal Method,” In: Yu. G. Shvartsman and I. N. Bolotov, Eds., *Natural Environment of the Solovetsky Archipelago under a Changing Climate*, The Ural Division of the Russian Academy of Sciences, Yekaterinburg, 2007, pp. 26-28.